

Physics Lab Report Title

Your Name

November 2, 2025

1 Introduction

Light, as a transverse electromagnetic wave, exhibits polarization when the oscillations of its electric field vector are confined to a specific plane perpendicular to the direction of propagation. While most natural light sources emit unpolarized light with random oscillation directions, polarization can be induced through transmission via polarizing materials or reflection at dielectric interfaces. This laboratory experiment investigates these phenomena using a low-powered red diode laser and Polaroid sheets to explore the transmission properties of polarized light and the partial polarization achieved by reflection. The primary objectives are threefold. First, Malus' law is verified by measuring the intensity of light transmitted through two successive polarizers as a function of the angle θ between their transmission axes, confirming the relationship $I(\theta) = I_0 \cos^2 \theta$. Second, the system is extended to three polarizers, with the first and third oriented at 90° to each other, to derive and test the intensity expression $I_3 = \frac{I_1}{4} \sin^2(2\phi)$, where ϕ is the angle of the intermediate polarizer relative to the first. Finally, polarization by reflection is examined at an air-acrylic interface to determine Brewster's angle θ_p , at which the reflected light is fully polarized perpendicular to the plane of incidence, enabling calculation of the refractive index of acrylic via $\tan \theta_p = n_2/n_1$. These exercises elucidate fundamental principles of wave optics, including the vector resolution of electric fields, intensity dependence on field amplitude, and the Fresnel equations governing reflectance for parallel ($R_{||}$) and perpendicular (R_{\perp}) polarizations. The results provide empirical validation of classical polarization theory and practical insight into applications such as glare reduction in polarized sunglasses.

2 Methodology

Describe experimental setup, equipment, and detailed procedure. Be specific enough that someone else could replicate the experiment.

3 Data and Analysis

3.1 Malus' Law

Collected data exhibits consistency and low uncertainty. Notably, at the start of each experiment, the rotary sensor must be pressed against the polarizer to prevent slipping; this procedure causes the rotary sensor to move around without changing the angle of the polarizer. Such error caused clusters of data points at maximum intensity and around $\theta = 0$.

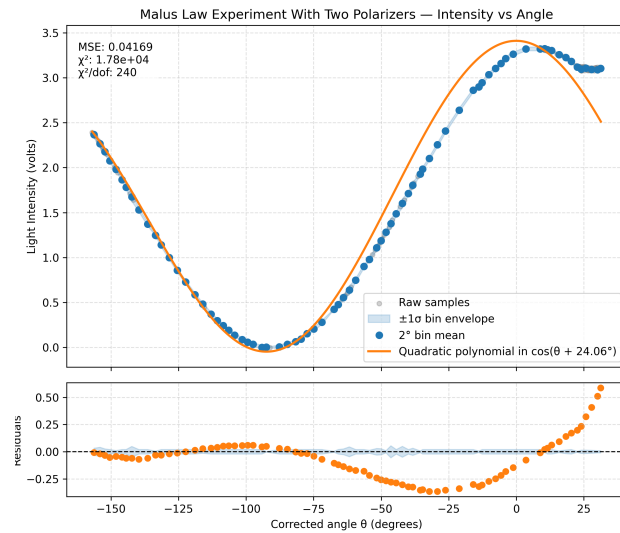


Figure 1: Intensity versus θ graph for two polarizers.

Data uncertainty is measured and reduced by combining a neighborhood of angles into bins of length 1° . The mean of the bin is plotted and areas one standard deviation from the mean is shaded. The cosine of the angles for two polarizers is fitted with a quadratic relationship with the intensity, While for three, a quartic relationship. The mean squared error and reduced χ^2 error for two polarizer are 0.04169 and 240.3, and for three polarizers, 0.002267 and 89.67, respectively.

Although the reduced chi squared error is much greater than one, indicating a poor model, the mean squared errors are small, showing a good fit. This

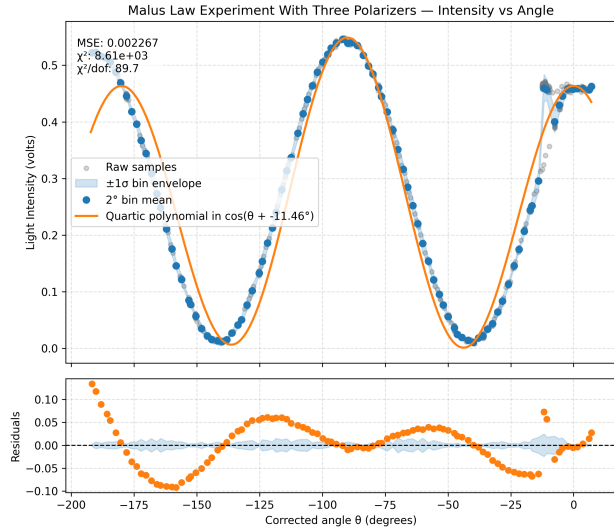


Figure 2: Intensity versus θ graph for three polarizers.

discrepancy can be attributed to the way standard deviation is calculated; because each bin contains few data points, it has small standard deviation. Since χ^2 error is very sensitive to data points with small standard deviations, even a small deviation from the fitted curve would contribute a lot to the χ^2 value.

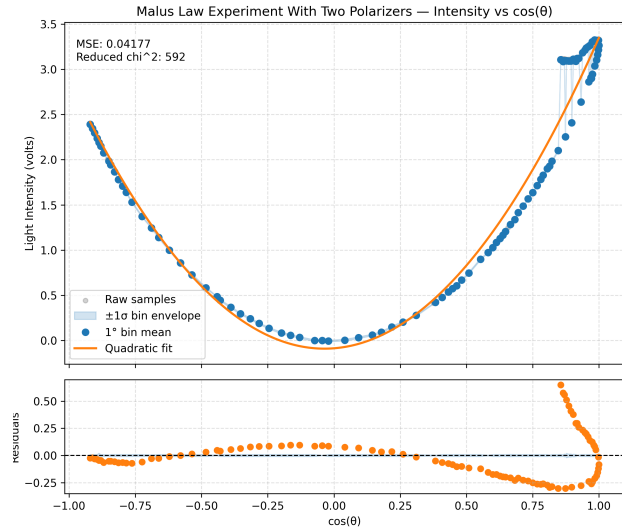


Figure 3: Intensity versus $\cos(\theta)$ graph for two polarizers. The uncertainty of the intensity and angle are invisible because the light sensor is accurate to a hundredth of a volt. The graph is roughly quadratic.

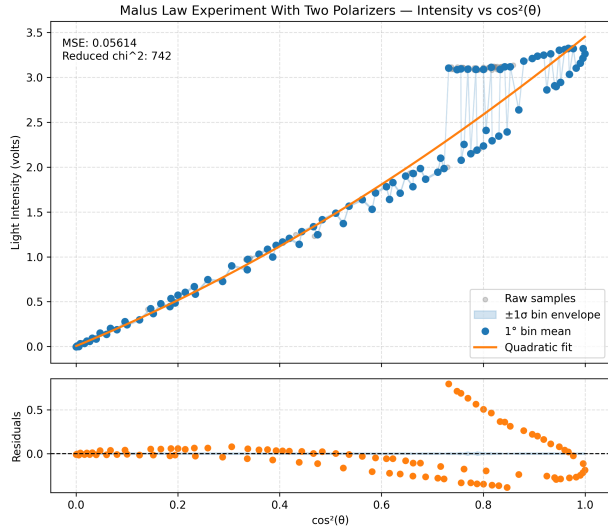


Figure 4: The light intensity is linear with $\cos^2 \theta$, with a mean squared error of 0.039. The two parallel but shifted patterns demonstrates that the rotary sensor has drift error possibly due to slip.

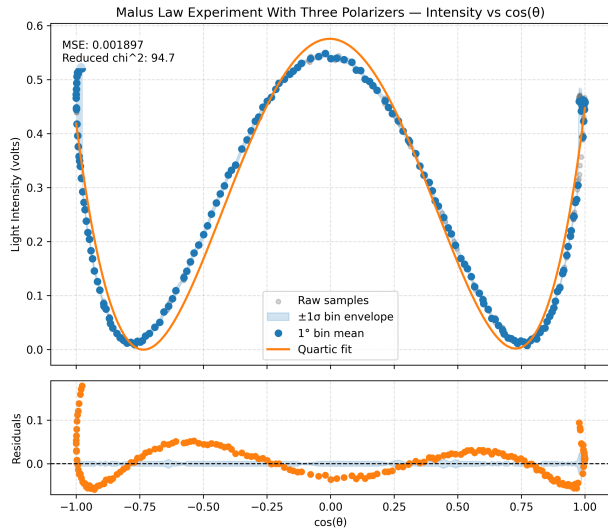


Figure 5: Intensity versus $\cos \theta$ graph for the three polarizers. The quartic curve has peaks at $\theta = 0^\circ, 90^\circ$, and 180° . Notably, the angle θ is offset by 45° from the real polarizer direction.

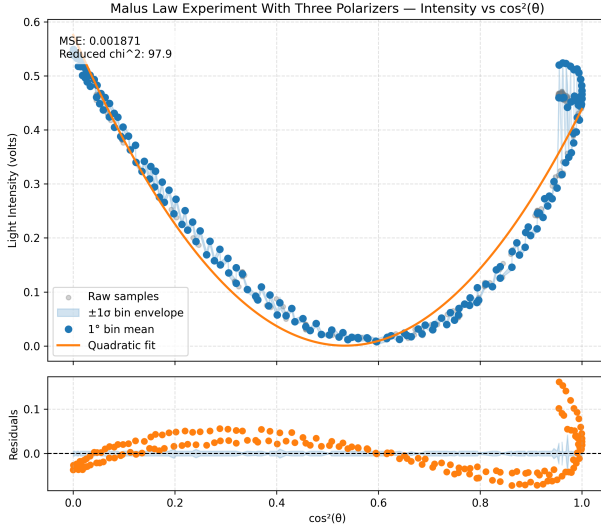


Figure 6: The intensity has a quadratic relationship with $\cos^2 \theta$, namely $I_3 = \frac{I_1}{2}(1 - \cos^2 \theta)(\cos^2 \theta)$, which can be derived from Eq.5 in the lab manual using trigonometric identities.

3.2 Brewster's Angle

The raw data obtained is very noisy due to the operation errors involved in rotating the apparatus disks concurrently. The light sensor is easily moved out of the way of the reflected light, causing sudden dips in intensity.

The sensor angle is offset by 70° from the incidence normal because the measurement software always begins recording at $\theta = 180^\circ$ but actual data collection begin at an angle from the incidence normal to not block the incident laser.

Notably, the error of both experiments grew larger with intensity. This could be attributed to error visibility, that when the actual intensity is near zero, an empty reading would not appear significant, but at high intensity, a dip in data differs greatly from the actual intensity.

Due to equipment limitations, the range of intensity recorded by the light sensor is constrained. To capture the small changes when intensity is low, the sensor must be amplified, which, however, overshoots intensity measurements at high intensity, causing clusters of data points at 4.3V, the maximum reading of the light sensor, around small reflection angles.

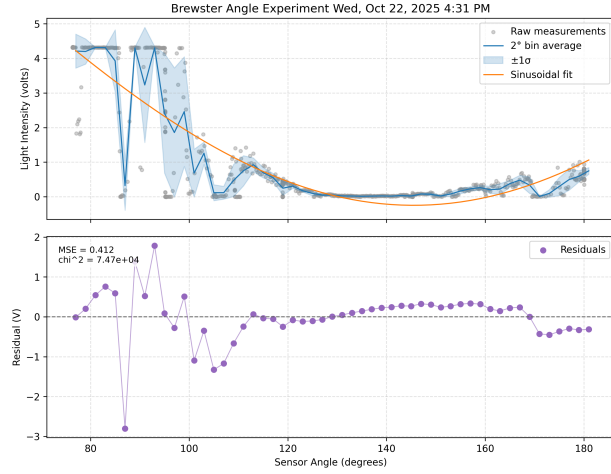


Figure 7: hiii

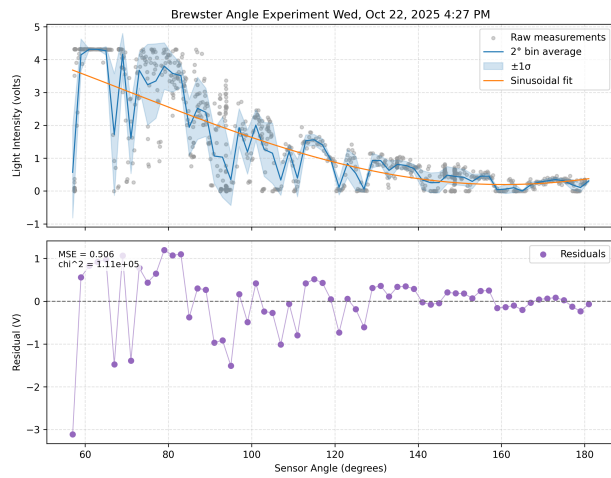


Figure 8: hiii

4 Discussion

5 Conclusion

Summarize findings, significance, and possible improvements for future work.

References

Use any citation style required (APA, MLA, etc.).